

Dual-Mode Reflectometer for Measuring Microwave Magnetic Kerr Effect in Semiconductors

PETER S. HAUGE, STUDENT, IEEE, AND KEITH S. CHAMPLIN, MEMBER, IEEE

Abstract—The “dual-mode reflectometer” is a device with which one can measure the relative off-diagonal terms of the tensor reflection coefficient of a hybrid mode composed of two degenerate, mutually perpendicular, independent modes. It differs from the conventional “single-mode reflectometer” in that it permits launching elliptically polarized waves of arbitrary orientation and ellipticity into the main (circular or square) waveguide and observing the orientation and ellipticity of the wave reflected by the load. This paper describes application of the dual-mode reflectometer to measurement of the magnetic Kerr effect in semiconductors. The accuracy and resolution of the apparatus is demonstrated with measurements of germanium and silicon at χ band. A scattering matrix analysis is given which describes the measurement and calibration procedure.

INTRODUCTION

WHEN a linearly polarized TE_{11}^0 wave propagates in a circular waveguide containing a longitudinally magnetized semiconductor, the direction of polarization is rotated and the wave becomes elliptically polarized. Rotation and change to elliptic polarization also occurs to the wave reflected by the interface between the empty and medium-filled waveguides. These phenomena are manifestations of the microwave Faraday [1] and magnetic Kerr [2] effects, respectively, and can be considered high-frequency analogs of the dc Hall effect. Analysis of either effect yields the relative off-diagonal term of the permittivity tensor of the material. The microwave Faraday effect has attracted recent interest as a tool for investigating scattering mechanisms and carrier inertia effects in semiconductors [3]–[5]. More recently the microwave magnetic Kerr effect has received attention [6]–[8]. There are several experimental conditions in which measurement of the magnetic Kerr effect may have advantages over measurement of the Faraday effect. Among these is the study of high-conductivity samples in which the transmitted wave may be greatly attenuated. Another is low-temperature studies requiring the sample to be placed in a cryogenic environment.

To measure the magnetic Kerr effect, an experimental means of separating the incident and reflected waves must be employed. An instrument utilizing a microwave turn-

stile junction has been used by Brodwin and Vernon [7] for this purpose. Their apparatus contains a balanced bridge circuit permitting precise null determination. Measurement accuracy depends on symmetry of both the turnstile junction and a hybrid junction used in the bridge. Rotations of the reflected wave of up to about 10 degrees can apparently be measured with high accuracy using their device.

This paper describes the use of a dual-mode reflectometer to separate incident and reflected waves. This device permits launching hybrid-mode TE_{11}^0 waves, (i.e., waves composed of two mutually perpendicular, independent, TE_{11}^0 modes) of arbitrary orientation and ellipticity into a circular waveguide and observing the orientation and ellipticity of the hybrid-mode wave returning from the load. In measuring the magnetic Kerr effect, the incident wave is actually adjusted to produce a linearly polarized reflected wave. This procedure, which is the reverse of a normal Kerr effect experiment, results in null output and yields high measurement precision.

Any asymmetry in components of the apparatus (e.g., waveguides, flange connections, transitions, coupling holes, etc.) is taken into account with six preliminary calibration measurements (see Appendix). Residual ellipticity caused by an asymmetrically-mounted sample is also taken into account. Thus, one need not assume conditions to be “ideal” in the experimental analysis. Measurements of Kerr effect rotation and ellipticity obtained with samples of *p*-type silicon and *n*-type germanium at low magnetic fields agree well with theory, thus lending support to the validity of the technique.

MICROWAVE APPARATUS

The dual-mode reflectometer is shown in Fig. 1. It is a 6-port device consisting of two TE_{10}^0 -mode rectangular waveguides coupled at right angles to a degenerate TE_{10}^0 -mode square waveguide by means of 20 dB directional couplers. Transitions from square to circular TE_{11}^0 -mode waveguide (not shown in Fig. 1) are attached at the top and bottom. A wave entering port 1 of the device excites a linearly polarized wave of the same orientation in the square waveguide and enters the transition to circular waveguide at port 3. Similarly, a wave entering port 2 excites a wave perpendicular to the first, entering the transition at port 4. The polarization and orientation of the resultant hybrid-mode TE_{11}^0 wave launched into the lower circular waveguide is thus determined by the relative magnitude and phase of the component waves entering ports 1 and 2. The hybrid wave re-

Manuscript received November 8, 1966; revised February 20, 1967. Research for this paper was sponsored by the U. S. Air Force Office of Scientific Research, Office of Aerospace Research, under Grant AF-AFOSR-606-67, and by the National Science Foundation under Grant GP-2360.

The authors are with the Dept. of Elec. Engrg., University of Minnesota, Minneapolis, Minn. 55455

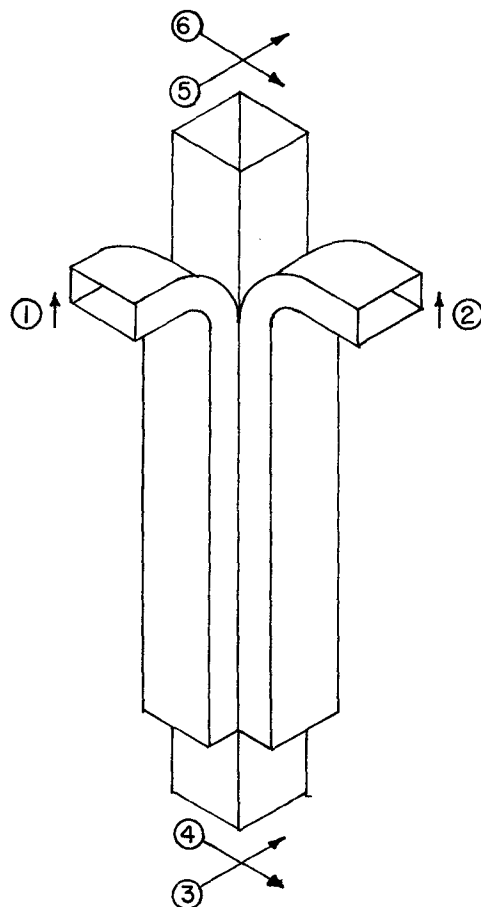


Fig. 1. The dual-mode reflectometer. The numbering of the ports and orientation of the degenerate modes of the square waveguide are shown. Transitions to circular guide (not shown) are placed at either end of the square guide.

flected by the load enters the transition to the upper circular waveguide at ports 5 and 6. It then passes through a rotating coupling and into a circular to rectangular transition (see Fig. 2) containing an absorbing vane parallel to the broad wall. The E -field component perpendicular to the vane excites a single TE_{10}^{\square} wave in the rectangular waveguide and is transmitted to a sensitive microwave receiver. By rotating the coupling, one can align the rectangular waveguide to receive any desired component of the elliptically polarized reflected wave. The vane absorbs the undesired orthogonal component.

The complete microwave circuit is shown in Fig. 3. A hybrid junction splits the signal from a frequency stabilized source into two independent waves. A precision attenuator and precision phase shifter control their relative magnitude and phase. The reflectometer combines them in space quadrature and illuminates the sample with the resultant hybrid wave. A null is observed at the receiver when the wave reflected by the sample is linearly polarized and oriented parallel to the absorbing vane in the upper rectangular waveguide.

To observe the Kerr effect, the attenuation A and phase ϕ are initially adjusted for null output with the magnetic field

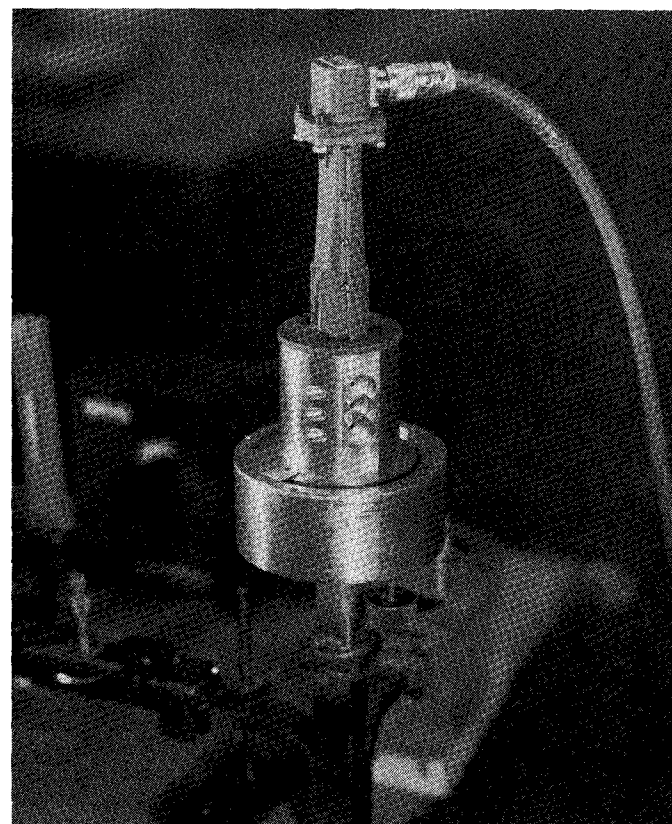


Fig. 2. The circular rotating coupling and circular to rectangular transition. Coaxial cable transmits signal to microwave receiver.

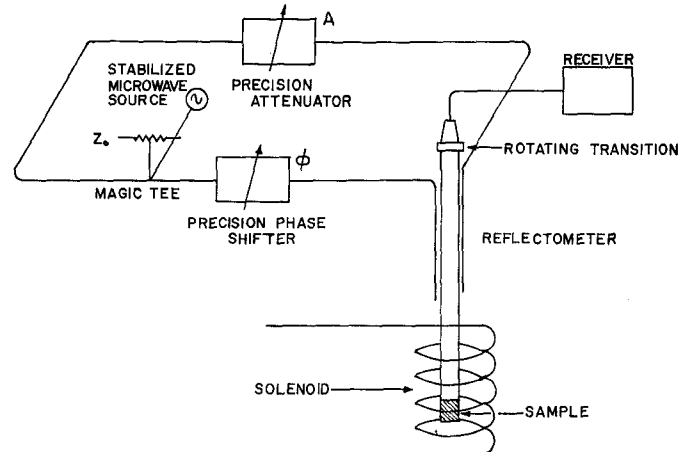


Fig. 3. Microwave circuit for observing microwave magnetic Kerr effect in semiconducting sample.

turned off. The sample is then magnetized, and A and ϕ are readjusted for null output. By noting the two values of A and ϕ , and the angle γ between the absorbing vane and port 6, one can calculate the Kerr effect produced by the sample. To indicate how this is done, we write the hybrid-mode reflection coefficient at the front surface of the sample in tensor form

$$\rho_{\text{sample}} = \rho_{33} \begin{bmatrix} 1 & \alpha - \beta \\ \alpha + \beta & 1 \end{bmatrix}. \quad (1)$$

Note that the off-diagonal elements contain both a symmetric and an antisymmetric term.¹ The symmetric term α , is associated with the residual ellipticity and rotation produced by any slight asymmetry in the sample mounting. The antisymmetric term β results from the Kerr effect and is an odd function of the magnetic field B . It can be shown that β is related to the Kerr effect rotation θ and ellipticity E (ratio of minor to major axes) produced by the sample by [7]

$$\theta = 1/2 \tan^{-1} \left[\frac{2|\beta| \cos \{\arg(\beta)\}}{1 - |\beta|^2} \right] \quad (2)$$

and

$$E = \left[\frac{1 + |\beta|^2 - D}{1 + |\beta|^2 + D} \right]^{1/2} \quad (3)$$

where

$$D = \{1 + 2|\beta|^2 \cos [2\{\arg(\beta)\}] + |\beta|^4\}^{1/2}. \quad (4)$$

For $|\beta| \ll 1$, (2) and (3) reduce to

$$\begin{aligned} \theta &= \operatorname{Re}(\beta) \\ E &= \operatorname{Im}(\beta) \end{aligned} \quad (5)$$

Because of unavoidable mechanical imperfections in the apparatus, the polarization direction and ellipticity observed a finite distance down the waveguide are generally not the same as those at the front surface of the sample. Furthermore, such spurious effects are not simply additive. For these reasons, the actual determination of β from measurements of γ , A , and ϕ involves two bilinear transformations using six constants found by preliminary calibration measurements. Details of this calculation and description of the calibration procedure are given in the Appendix.

As with single-mode reflectometers [9], directivity and matching conditions must be satisfied if one is to avoid certain measurement errors. They are:

1) The couplers should have sufficient directivity to make back coupling negligible.

2) Ports 3 and 4 should be matched looking away from the sample.

If necessary, one may obtain these conditions with small tuning stubs adjusted by techniques similar to those used with a single-mode reflectometer [9]. The couplers for this experiment were designed to have infinite directivity [10] at the operating frequency, however, and the directivity was found experimentally to be larger than 50 dB. Furthermore, it was found unnecessary to use tuning stubs to obtain a good match at ports 3 and 4.

EXPERIMENTAL RESULTS

In order to demonstrate the utility of the apparatus, the results of two experiments are described. These results are typical of many Kerr effect measurements made on silicon

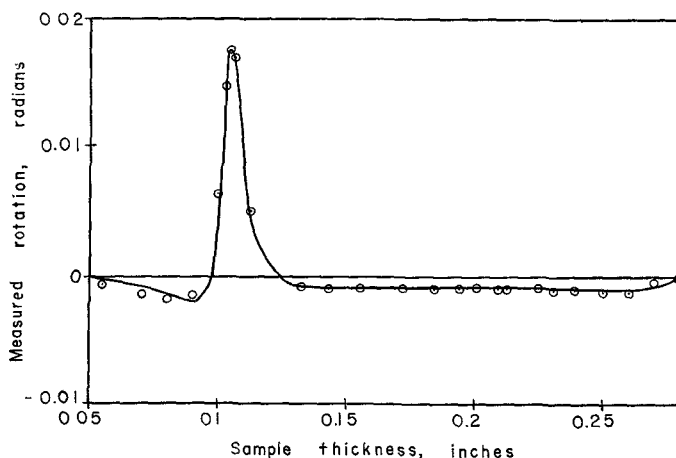


Fig. 4. Kerr rotation versus sample thickness for $60\Omega\cdot\text{cm}$ *p*-type silicon. Data points are experimental and curves are calculated (see text). Magnetic field is 0.327 W/m^2 .

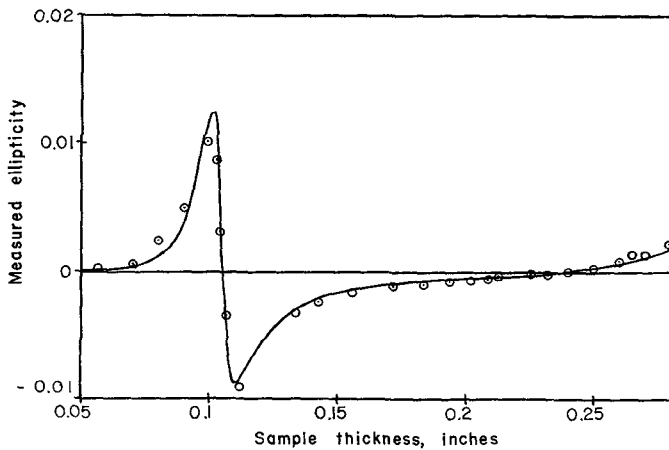


Fig. 5. Kerr ellipticity versus sample thickness for $60\Omega\cdot\text{cm}$ *p*-type silicon. Data points are experimental and curves are calculated (see text). Magnetic field is 0.327 W/m^2 .

and germanium samples at room temperature and at the temperature of liquid nitrogen. In all cases, the sample completely filled the circular waveguide and was backed up by a short circuit.

Figures 4 and 5 show the effect of sample thickness on Kerr effect rotation and ellipticity for a $60 \Omega\cdot\text{cm}$ *p*-type silicon sample at room temperature and constant magnetic field of 0.327 W/m^2 . These data were obtained by lapping the sample in steps of about 0.010 inch between successive measurements. The thickness corresponding to maximum rotation is approximately $(\lambda_g/4)$ where λ_g is the guide wavelength in the silicon-filled waveguide. Theoretical curves plotted in Figs. 4 and 5 were obtained by evaluating the complex derivative of the reflection coefficient with respect to the propagation coefficient of the sample with a digital computer [5]. The conductivity and permittivity used in these calculations were actual measured values obtained with a microwave reflection coefficient bridge [11]. Excellent agreement between theory and experiment is noted.

¹ The form of the off-diagonal elements follows from the reciprocity theorem (Onsager relations).

The second experiment to be described used the magnetic Kerr effect to determine the room-temperature Hall mobility [5] of a $4\Omega\cdot\text{cm}$ sample of *n*-type germanium. At room temperature, inertial effects are negligible at *x* band so that the microwave Hall mobility $\hat{\mu}_H$ is a real quantity. Thus, Kerr effect rotation and ellipticity are redundant and one should be able, in principle, to determine $\hat{\mu}_H$ from either quantity [5]. For a sample 0.0856 inch thick, the following experimental values were obtained:

$$\begin{aligned}\theta &= -0.00675 \text{ rad}, \\ E &= -0.00103, \text{ and} \\ B &= 0.218 \text{ W/m}^2.\end{aligned}$$

By combining these data with microwave conductivity and permittivity measured with a reflection coefficient bridge [11] the following two values of $\hat{\mu}_H$ were calculated,

$$\begin{aligned}\text{from rotation } \hat{\mu}_H &= -0.325 \text{ m}^2/\text{V}\cdot\text{s}, \text{ and} \\ \text{from ellipticity } \hat{\mu}_H &= -0.310 \text{ m}^2/\text{V}\cdot\text{s}.\end{aligned}$$

One sees that these values agree very closely with one another. Furthermore, they both agree fairly well with the value of dc Hall mobility

$$\mu_H = -0.35 \text{ m}^2/\text{V}\cdot\text{s}$$

measured on a sample having similar resistivity by Debye and Conwell [12] using traditional dc Hall effect techniques.

CONCLUSIONS

The dual-mode reflectometer is seen to be a practical device for studying the tensor reflection coefficient of a hybrid mode composed of two degenerate, mutually perpendicular, independent modes. Such hybrid modes are dominant in waveguides possessing 90 degree rotational symmetry (such as, e.g., circular or square waveguides). The device can be analyzed (see Appendix) by an extension of the theory of the single-mode reflectometer.

One use for the dual-mode reflectometer is measurement of the magnetic Kerr effect in semiconductors. This effect is manifested by a change in polarization and ellipticity of a hybrid mode as it is reflected from the surface of a longitudinally magnetized sample. Measurements of these changes can be used to determine the real and imaginary parts of the complex off-diagonal term of the permittivity tensor [5]. In the region $\omega\tau \ll 1$ (room temperature, *x* band) where the off-diagonal term is pure imaginary [5], Kerr effect rotation and ellipticity are redundant and contain the same information as the dc Hall effect. For larger values of $\omega\tau$, however, additional information about the energy bands and scattering mechanisms is conveyed. Microwave magnetic Kerr effect studies at cryogenic temperatures should therefore prove useful in extending knowledge of the behavior of electrons in semiconductors.

APPENDIX

The purpose of this appendix is to analyze the dual-mode reflectometer, and describe how it can be calibrated. We will assume that ports 3 and 4 and the rotating transition on

ports 5 and 6 of the reflectometer are matched, and that the directional couplers are sufficiently directive that back coupling is negligible. The scattering matrix equation of the reflectometer is then of the form

$$\begin{bmatrix} b_1 \\ b_2 \\ b_3 \\ b_4 \\ b_5 \\ b_6 \end{bmatrix} = \begin{bmatrix} S_{11} & S_{12} & S_{13} & S_{14} & 0 & 0 \\ S_{12} & S_{22} & S_{23} & S_{24} & 0 & 0 \\ S_{13} & S_{23} & 0 & 0 & S_{35} & S_{36} \\ S_{14} & S_{24} & 0 & 0 & S_{45} & S_{46} \\ 0 & 0 & S_{35} & S_{45} & S_{55} & S_{56} \\ 0 & 0 & S_{36} & S_{46} & S_{56} & S_{66} \end{bmatrix} \begin{bmatrix} a_1 \\ a_2 \\ a_3 \\ a_4 \\ 0 \\ 0 \end{bmatrix}. \quad (6)$$

For convenience, we define the following complex ratios of perpendicular modes:

$$R_1 \equiv 10^{-A/20}/\exp[-j\phi] \equiv c(a_1/a_2) \quad (7)$$

$$R_2 \equiv b_3/b_4 \quad (8)$$

$$R_3 \equiv a_3/a_4 \quad (9)$$

$$R_4 \equiv b_5/b_6 \quad (10)$$

where *c* is a complex constant, *A* is the setting of the precision attenuator in decibels, and ϕ is the setting of the precision phase shifter in radians. The scattering matrix equation of the sample terminating ports 3 and 4 can be written as

$$\begin{bmatrix} a_3 \\ a_4 \end{bmatrix} = \rho_{33} \begin{pmatrix} 1 & \rho_{34}' \\ \rho_{43}' & 1 \end{pmatrix} \begin{bmatrix} b_3 \\ b_4 \end{bmatrix}. \quad (11)$$

Let γ be the angle between the absorbing film in the rotating transition and the *E* field of port 6. At null output R_4 is real, and one can write

$$R_4 = \tan \gamma. \quad (12)$$

By substituting (7) through (12) into the expressions for b_3-b_6 obtained from (6), one obtains the following null relations

$$\begin{aligned}R_2 &= \frac{(S_{13}/c)R_1 + S_{23}}{(S_{24}/c)R_1 + S_{24}} \\ &\equiv \frac{C_1 R_1 + C_2}{C_3 R_1 + 1},\end{aligned} \quad (13)$$

$$R_3 = \frac{R_2 + \rho_{34}'}{\rho_{43}' R_2 + 1}, \quad (14)$$

and

$$\begin{aligned}\tan \gamma &= \frac{S_{35}R_3 + S_{45}}{S_{36}R_3 + S_{46}} \\ &\equiv \frac{C_4 R_3 + C_5}{C_6 R_3 + 1}.\end{aligned} \quad (15)$$

The calibration constants C_1-C_6 can be determined as follows: the rotating transition is removed from ports 5 and 6 and placed on ports 3 and 4; the condition for null then becomes

$$R_2 = \tan \gamma. \quad (16)$$

Null output is obtained for three values of γ by adjusting A and ϕ . Using these data, (7), (13), and (16) are solved to obtain C_1-C_3 . The rotating transition is returned to ports 5 and 6, and ports 3 and 4 are short circuited so that $\rho_{34}' = \rho_{43}' = 0$. Again, A and ϕ are adjusted for null output at three values of γ . Using these data and values of C_1-C_3 previously determined, (7) and (11) through (15) are combined to yield C_4-C_6 . The apparatus is now calibrated.

To measure Kerr effect, a sample is placed at ports 3 and 4, and the off-diagonal terms in (11) become

$$\left. \begin{aligned} \rho_{34}' &= \alpha - \beta \\ \rho_{43}' &= \alpha + \beta \end{aligned} \right\}. \quad (17)$$

With the rotating transition set at some arbitrary angle γ , A and ϕ are adjusted for null output with and without the applied magnetic field B . Inserting those values of A and ϕ into (7) and (13) yields two values of R_2 . The single value R_3 is found from γ with (15). Equation (14) evaluated with and without the magnetic field thus becomes

$$R_3 = \frac{R_2(0) + \alpha}{\alpha R_2(0) + 1} \quad (18)$$

and

$$R_3 = \frac{R_2(B) + \{\alpha - \beta\}}{\{\alpha + \beta\}R_2(B) + 1}. \quad (19)$$

The magnetic Kerr effect follows by solving (18) and (19) simultaneously for β . Although calculation of the preceding equations is straightforward, it is fairly time consuming. For this reason, we have programmed a digital computer to

determine β directly from the calibration and measurement data obtained from the apparatus.

REFERENCES

- [1] M. Faraday, "On the magnetic affection of light and on the distinction between the ferromagnetic and diamagnetic conditions of matter," *Philos. Mag.*, vol. 29, ser. 3, pp. 153-156, September 1846.
- [2] J. Kerr, "On rotation of the plane of polarization by reflection from the pole of a magnet," *Philos. Mag.*, vol. 3, ser. 5, pp. 321-342, May 1877. Also, J. Kerr, "On reflection of polarized lights from equatorial surface of a magnet," *Philos. Mag.*, vol. 5, ser. 5, pp. 161-177, March 1878.
- [3] R. R. Rau and M. E. Caspary, "Faraday effect in germanium at room temperature," *Phys. Rev.*, vol. 100, pp. 632-639, June 1955.
- [4] J. K. Furdyna and S. Broersma, "Microwave Faraday effect in silicon and germanium," *Phys. Rev.*, vol. 120, pp. 1995-2003, December 1960.
- [5] K. S. Champlin and D. B. Armstrong, "Waveguide perturbation techniques in microwave semiconductor diagnostics," *IEEE Trans. Microwave Theory and Techniques*, vol. MTT-11, pp. 73-77, January 1963.
- [6] M. E. Brodwin, J. K. Furdyna, and R. J. Vernon, "Free-carrier magneto-Kerr effect in semiconductors," *Bull. Am. Phys. Soc.*, vol. 6, p. 427, December 1961.
- [7] M. E. Brodwin and R. J. Vernon, "Instrument for measuring the magneto-microwave Kerr effect in semiconductors," *Rev. Sci. Instr.*, vol. 34, pp. 1129-1132, October 1963.
- [8] —, "Free-carrier magneto-microwave Kerr effect in semiconductors," *Phys. Rev.*, vol. 140, pp. A1390-A1400, November 1965.
- [9] G. F. Engen and R. W. Beatty, "Microwave reflectometer techniques," *IRE Trans. Microwave Theory and Techniques*, vol. MTT-7, pp. 351-355, July 1959.
- [10] E. S. Hensperger, "The design of multi-hole coupling arrays," *Microwave J.*, vol. 2, pp. 38-42, August 1959.
- [11] K. S. Champlin, D. B. Armstrong, and P. D. Gunderson, "Charge carrier inertia in semiconductors," *Proc. IEEE*, vol. 52, pp. 677-685, June 1964.
- [12] P. P. Debye and E. M. Conwell, "Electrical properties of *n*-type germanium," *Phys. Rev.*, vol. 93, pp. 693-706, February 1954.

On the Theory of Shielded Surface Waves

JAMES R. WAIT, FELLOW, IEEE

Abstract—An analysis is given for the modes which will be excited between two parallel impedance boundaries. It is shown that, for inductive-type surfaces, two of these modes have a surface wave character even though the structure is bounded in the transverse dimension. The interaction between these surface waves and the accompanying waveguide modes is discussed for this model which is admittedly highly idealized.

Manuscript received September 9, 1966; revised January 23, 1967.

The author is with the Institute for Telecommunication Sciences and Aeronomy, Environmental Science Services Administration, Boulder, Colo. 80302.

INTRODUCTION

IN A RECENT interesting paper, Barlow [1] has considered the possibility that a surface wave may be shielded in such a manner that its transverse field pattern is limited. He proposed the application of the concept to communication circuits for high-speed trains. The main advantage would be its insensitivity to outside interference.

In order to provide further insight into the nature of shielded surface waves, a rather simple model is chosen here.